Characterizing Barium Titanate Piezoelectric Material Using the Finite Element Method

Zubair Butt[†] and Shafiq Ur Rahman
Department of Mechatronics Engineering, Chakwal Campus, University of Engineering and Technology Taxila, Chakwal 48800, Pakistan

Riffat Asim Pasha, Shahid Mehmood, and Saqlain Abbas
Department of Mechanical Engineering, University of Engineering and Technology Taxila, Taxila 47080, Pakistan

Hassan Elahi
Department of Aerospace Engineering, La Sapienza University of Rome, Rome 00145, Italy

The aim of the current research was to develop and present an effective methodology for simulating and analyzing the electrical and structural properties of piezoelectric material. The finite element method has been used to make precise numerical models when dielectric, piezoelectric and mechanical properties are known. The static and dynamic responses of circular ring-shaped barium titanate piezoelectric material have been investigated using the commercially available finite element software ABAQUS/CAE. To gain insight into the crystal morphology and to evaluate the purity of the material, a microscopic study was conducted using a scanning electron microscope and energy dispersive x-ray analysis. It is found that the maximum electrical potential of 6.43 V is obtained at a resonance frequency of 35 Hz by increasing the vibrating load. The results were then compared with the experimentally predicted data and the results agreed with each other.

Keywords: Barium titanate, Finite element method, Static analysis, Dynamic analysis, SEM

1. INTRODUCTION

Piezoelectric materials contain a crystalline structure that gives them the ability to convert strain energy produced by applied mechanical force into electrical potential and vice versa. Energy harvesting refers to the methods used to obtain and convert the energy surrounded by a system into useful electrical energy [1]. In recent decades, there has been much research in the field of power harvesting. The developments in this research have revolutionized wireless technology and electronic devices

such as microelectromechanical systems. Despite other sources of energy harvesting such as electromagnetic generation and electrostatic generation, piezoelectric materials offer promising potential as ideal sources. In 2011, a study was conducted for vibration-based energy harvesting using a clamped piezoelectric circular diaphragm. A power output of 12 mW was obtained at the harvester's resonance frequency (113 Hz) using a 33 kΩ resistor at a load of 1.2 N and acceleration of 9.8 m/s². With the increase in pre-stressing, energy harvested increases with decreased resonance frequency [1,2]. In 2014, an investigation was conducted to harvest energy over a wide range of frequencies by developing a piezoelectric generator using multiple circular piezoelectric harvester arrays. A power output of 11 mW was obtained under a load of 0.15 N at the resonance frequency of 590 Hz using a piezoelectric drum transducer and an 18 kΩ resistor [3]. There have been numerous opportunities to harvest power in sensible real-world applications with the help of this advanced research.

[†] Author to whom all correspondence should be addressed:
E-mail: zubairbutt64@yahoo.com

164

Trans. Electr. Electron. Mater. 18(3) 163 (2017): Z. Butt *et al.*

Piezoelectric sensors based on the ambient vibrations that surround a system have triggered reasonable increases in their use for energy harvesting. This property enhances the ability of these materials to absorb the mechanical energy available in the form of ambient vibrations surrounding a system and change it into the electrical charges that power different electronic devices [4,5]. Finite element (FE) based numerical simulations using standard software packages such as ABAQUS are useful tools for solving and verifying practical engineering problems in diverse fields such as thermal, fluid, piezoelectric and structural analysis [6,7]. The piezoelectric effect is a coupled interface between a material's electrical field and structural distortion. Today, the FE method to perform the static and dynamic analysis of coupled field piezoelectric material is available in some commercial packages, and the coupled field elements required for the piezoelectric effect have been used in finite element analysis. Coupled field elements involve electrical and structural coupling in element matrices and also comprise all necessary nodal degrees of freedom [8]. FEA (finite element analysis) is very attractive for modeling piezoelectric sensors and actuators [9]. A. H. Allik presented the first numerical simulation of piezoelectric material in 1970 [10]. R. Lerch performed time domain modeling and transient analysis of piezoelectric material under mechanical loading using the finite element method [11]. Der Ho Wu studied the harmonic response and resonance frequency of a piezoelectric plate using coupled-field FEA [12]. The output power of piezoelectric energy harvester plates was also predicted with an electromechanical coupled FE model; the goal was to power small electronic devices by transforming the waste vibration energy available in the atmosphere into electrical energy [13]. The advantage of FEA over analytical results is that mechanical stress variations and electrical field calculations of complex geometries of the material can be more readily calculated. FEA was performed to calculate the stress and electric field distributions under static loads and under any electrical frequency, and thus, the impact of material geometry can be evaluated and improved without the need to make and test various materials. In addition, FEA can likely predict lifetime expectations without the need to conduct time-consuming tests if the significant electrical and mechanical parameters are obtained [14].

Our aim in this study was to investigate whether 3D electromechanical coupled-field FEA could be used to accurately predict the behavior of piezoelectric material. In this paper, we clarify the details of how we constructed a finite element model for piezoelectric material. We investigated the voltage response of circular ring-shaped barium titanate (BaTiO₃) piezoelectric material under static and dynamic loading using the commercially available FE software ABAQUS™ Standard. In order to validate the model, we experimentally measured the voltage response of the piezoelectric material and compared it with that predicted by the FE method.

In addition, we conducted microstructure analysis of this material using scanning electron microscopy (SEM), and we performed energy-dispersive x-ray analysis (EDX) to determine the chemical composition of this material before we began the experimental work.

2. METHODOLOGY OF RESEARCH

2.1 Finite element electromechanical field equations

Piezoelectric materials exhibit elastic behavior, and defining those properties correctly controls the performance of piezoelectric material in a particular direction [15]. The governing equations used to represent the linear behavior of piezoelectric in FEM software are:

$$T = C_E S - eE \tag{1}$$

$$D = e^T S + \varepsilon_s E \tag{2}$$

Where T = the stress vector, D = the electric flux density vector, S = the strain vector, E = the electric field vector, C_E = the elasticity matrix, e = the piezoelectric stress matrix, and ε_s= the dielectric matrix at constant mechanical strain. An anisotropic symmetric and un-inverted matrix form [C] can be used to represent the elasticity matrix C as shown in equation (3):

$$C_E = \begin{bmatrix} c_{11} & c_{12} & c_{13} & c_{14} & c_{15} & c_{16} \\ c_{21} & c_{22} & c_{23} & c_{24} & c_{25} & c_{26} \\ c_{31} & c_{32} & c_{33} & c_{34} & c_{35} & c_{36} \\ c_{41} & c_{42} & c_{43} & c_{44} & c_{45} & c_{46} \\ c_{51} & c_{52} & c_{53} & c_{54} & c_{55} & c_{56} \\ c_{61} & c_{62} & c_{63} & c_{64} & c_{65} & c_{66} \end{bmatrix} \tag{3}$$

The elasticity matrix determined at constant electric flux density C_D can be used for the input, and it is given by equation (4):

$$C_D = C_E + \frac{e^2}{\varepsilon_s} \tag{4}$$

The piezoelectric stress matrix e, which relates the electric field vector E in the order x, y, z to the stress vector T in the order x, y, z, xy, yz, xz and has the form:

$$e = \begin{bmatrix} e_{11} & e_{12} & e_{13} \\ e_{21} & e_{22} & e_{23} \\ e_{31} & e_{32} & e_{33} \\ e_{41} & e_{42} & e_{43} \\ e_{51} & e_{52} & e_{53} \\ e_{61} & e_{62} & e_{63} \end{bmatrix} \tag{5}$$

The piezoelectric matrix e is also related to piezoelectric strain matrix d by the relationship given in equation (6):

$$e = c.d \tag{6}$$

The variable ε_s uses electrical permittivity and can be represented in either its orthotropic or anisotropic forms as:

$$\varepsilon_s = \begin{bmatrix} \varepsilon_{11} & 0 & 0 \\ 0 & \varepsilon_{22} & 0 \\ 0 & 0 & \varepsilon_{33} \end{bmatrix} \tag{7}$$

The dielectric matrix at constant stress ε_T can be converted into a dielectric matrix at constant strain ε_s using the following equation:

$$\varepsilon_s = \varepsilon_T - e^T d \tag{8}$$

Developing the nodal solution variables and element shape functions for an element domain to approximate the solution defines the finite element discretization as:

$$U_C = N^T{}_U . U \tag{9}$$

$$V_C = N_V . V \tag{10}$$

Where U_C = the displacement in the element domain within the given coordinates, V_C = the electrical potential, N_U = the matrix of the displacement shape functions, N_V = the vector of the electrical potential shape function, U = the vector of the nodal displacements, and V = the vector of nodal electrical potential.

2.2 Finite element simulation

The piezoelectric effect is a dilatational effect in which there is no rotation and shear in a material principle coordinate system [19]. We developed a three-dimensional (3D), deformable, ring-

Trans. Electr. Electron. Mater. 18(3) 163 (2017): Z. Butt *et al*.

165

shaped finite element model for BaTiO$_3$ piezoelectric materials in ABAQUS/CAE software to analyze the effects of static and dynamic loadings. The model had a thickness of 4 mm, with inner and outer diameters of 12 mm and 23 mm, respectively, similar to those of the specimens we used during the experimentation. The aim of this study was to determine the actuator's peak voltage over a range of frequencies using FE analysis. We used a full Newton integration scheme in ABAQUS to design the model geometry of the material. The final meshed model of the BaTiO$_3$ material consisted of 11672 hexahedral C3D8E elements and 14130 nodes. We applied a constant load at the upper surface of the piezoelectric material along the polarization directions. The top surface was made at zero charge/symmetry, and the bottom surface of the material was grounded. We conducted general static and dynamic analyses while applying a uniformly distributed load at the upper surface of the material, and we obtained the corresponding electrical potential (EPOT) and compared it with the experimental data. Fig. 1 shows the meshed BaTiO$_3$ model in which both the polarization and displacement directions are aligned. Table 1 shows the related mechanical properties for this material provided by the supplier with reference to [20].
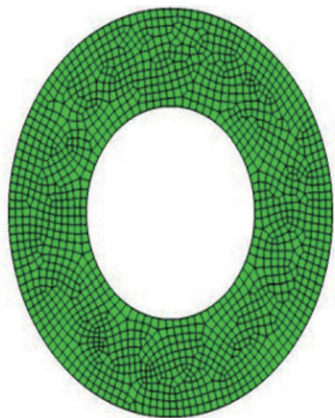

Fig. 1. Meshed model of ring-shaped BaTiO$_3$ with global size of 0.0005.

Table 1. Mechanical and piezoelectric properties of the material used in ABAQUS [20].

Mechanical Properties	BaTiO$_3$
Density (kg/m^3)	5600
Elastic coefficient (GPa)	
C$_{11}$	166
C$_{23}$	0
C$_{12}$	76.6
C$_{13}$	77.50
C$_{33}$	162.0
C$_{44}$	42.90
C$_{66}$	0
Piezoelectric coupling coefficient (10^{-12} m/V)	
d$_{15}$	150
d$_{31}$	-33
d$_{33}$	82
Piezoelectric coefficient (C/m²)	
e$_{13}$	0
e$_{15}$	11.60
e$_{31}$	-4.40
e$_{33}$	18.60
e$_{52}$	0
Dielectric constant (10^{-9} F/m)	
ε_{11}	11.151
ε_{22}	0
ε_{33}	12.567

2.3 Experimental procedure

We also verified the simulation results by developing an experimental setup. In the present study, we selected a circular ring-shaped BaTiO$_3$ piezoelectric material, provided by a supplier (Piezo Systems, Inc. USA), for experimentation because of its low energy loss characteristics. The BaTiO$_3$ material is the first known ferroelectric ceramic and can be prepared using different methods depending on the desired characteristics; it can be manufactured by the comparatively simple sol–hydrothermal method, and it can also be formed by heating barium carbonate and titanium dioxide. The material has a variety of applications resulting from its excellent dielectric, ferroelectric, and piezoelectric properties, and because of its low loss characteristic, it is an excellent choice for many applications such as capacitors and energy storage devices [21]. The ring has a thickness of 4mm, with an inner and outer radius of 6 mm and 11.5 mm, respectively. The ring was poled in the thickness direction, and copper electrodes were coated on two major surfaces of the ring. The piezoelectric ring has a charge constant (d33) of 82×10^{-12} m/V and the Curie temperature is 550℃. It is well-known that under resonant vibration, the relative displacement of piezoelectric rings considerably improves, and we obtained the maximum electrical potential at its resonance frequency.

Figure 2 shows the measurement setup we used to harvest energy during the current research work. We used the function generator (HAMEG-8150) to measure the performance of the commercial piezo ring at various sinusoidal frequencies and voltage amplitudes and a 25 N electromagnetic shaker (Model-F10/Z820WA) with a wide frequency range to provide sinusoidal vibrating load conditions so that we could measure the dynamic and static responses of the material. We monitored the applied load using a load cell (HYTEK) placed at the bottom layer of the specimen. We also used an impedance analyzer (HP-4294A) connected with a switch box circuit to measure the impedance, resonance, and anti-resonance frequency. We prepared an oscillator circuit to produce a very low distortion frequency signal and used a simple energy harvesting circuit (AC to DC converter) to measure the DC voltage across the harvester.

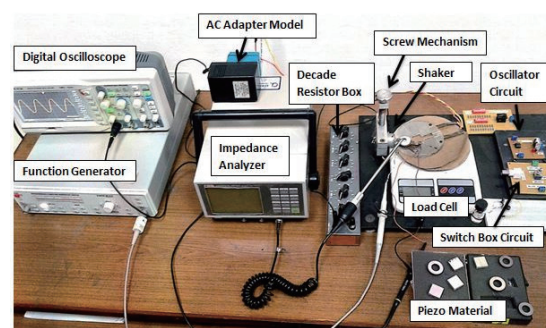Figure 3 shows a rectifier circuit consisting of four diodes

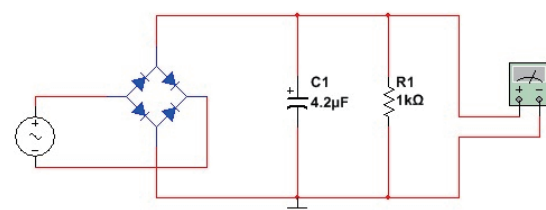Fig. 2. Experimental setup used to harvest the energy.

Fig. 3. Schematic diagram of the energy-harvesting circuit.

connected to the piezoelectric ring. To measure the current through the ring, we stored in a capacitor a 1 kΩ resistor connected in series and the generated electrical potential. To avoid any noise or other adjacent environment effects, we placed the experimental setup on an insulated bench and monitored the dynamic and static response of the piezoelectric material on a digital oscilloscope (GPS-1072B).

2.3 Scanning electron microscopy

Piezoelectric materials have been applied in electromechanical devices as sensors and actuators. These materials contain many microscopic crystal grains and domains. Because of their asymmetrical crystal structures, such as cubic, tetragonal, and rhombohedran, all domains display anisotropic mechanical and electrical behaviors, and the macroscopic properties of these materials rely heavily on this microscopic crystal morphology. Therefore, it is essential to study the microstructural characteristics of these polycrystalline materials using SEM and EDX [16,17]. Scanning electron microscopes use concentrated beam of electrons that by interacting with materials at their atomic levels produce signals regarding the materials' surface composition and topography to generate microscopic images [18,22].

3. RESULTS AND DISCUSSION

3.1 Crystal morphology and microstructure

We conducted microstructure and morphological observation of ring-shaped polycrystalline $BaTiO_3$ piezoelectric material using SEM (VEGA3-TESCAN) at 10.0 kV. The specimen was electrically poled in the thickness direction and had inner and outer radiuses of 6 mm and 11.5 mm, respectively. The material has a perovskite tetragonal structure, and we set the scanning interval to 16.8 μm. We crackled the specimen with a thin gold layer in the evaporator before scanning in order to avoid charging the electrons.

Figure 4 shows the crystal morphology of this material. We observed that the crystal grains were highly agglomerated, with large particles due to overlapping that combined with small particles. The figure shows the varied scattering of grains all over the substrate.
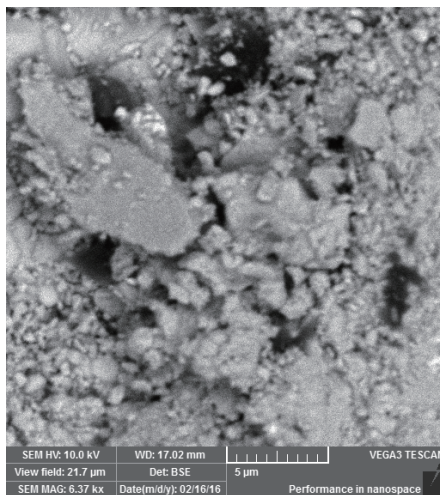

Fig. 4. Crystal morphology of material.

3.2 Energy dispersive X-ray analysis (EDX)

We performed EDX analysis to determine the atomic

percentages of Ba, Ti, and O at different randomly selected locations on the specimen. For this reason, we polished the surface of the $BaTiO_3$ material with CAMI grade 1000 sandpaper with average element size in micron inches. After the fine polishing, we placed the material under the SEM to perform the chemical analysis.

Figure 5 shows the three different spectrums with grain size of 10 μm in order to determine the composition of this material. The Ba:Ti:O concentration ratio shows that the material was sub-stoichiometric in nature. Figures 6, 7, and 8 show the relative quantities of the Ba, Ti, and O. The figures show clearly that there were no impurities, which indicates the high purity of the material we selected for the required experimentation. Table 2 shows the experimental values of $BaTiO_3$ obtained from the three different EDX spectrums.
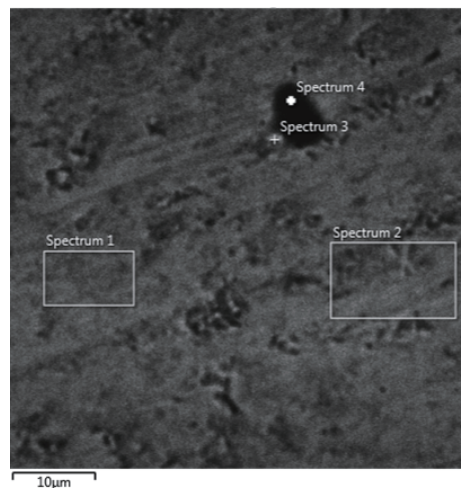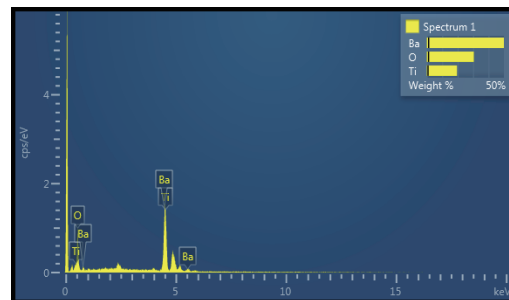

Fig. 5. Electron image of $BaTiO_3$.

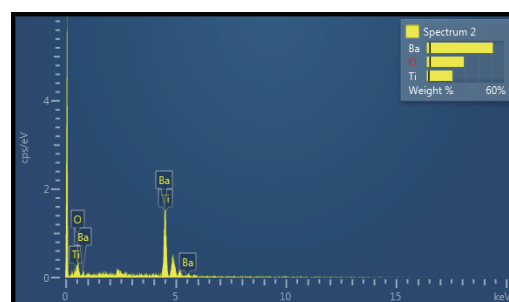Fig. 6. Weight percentages of the elements in $BaTiO_3$ at spectrum 1.

Fig. 7. Weight percentages of the elements in $BaTiO_3$ at spectrum 2.

Trans. Electr. Electron. Mater. 18(3) 163 (2017): Z. Butt *et al*.
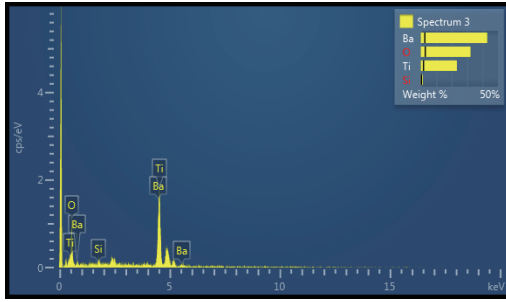
167

Fig. 8. Weight percentages of the elements in BaTiO$_3$ at spectrum 3.

Table 2. Atomic % of Ba, Ti and O obtained from EDX.

Region	Atomic %		
	Ba	Ti	O
Spectrum 1	50	14	36
Spectrum 2	60	15	25
Spectrum 3	50	20	30

3.3 Static analysis

Initially, we conducted a general static analysis that entailed applying uniformly distributed loads that varied from 1 to 150 kN/m^2 to the top surface of the piezoelectric material. Once we applied the load, the material was electrically polarized, and the polarization varied directly with the applied load. The nodal solution of the EPOT variations in the material, derived from ABAQUS, is shown in Fig. 9, and Fig. 10 shows the experimental
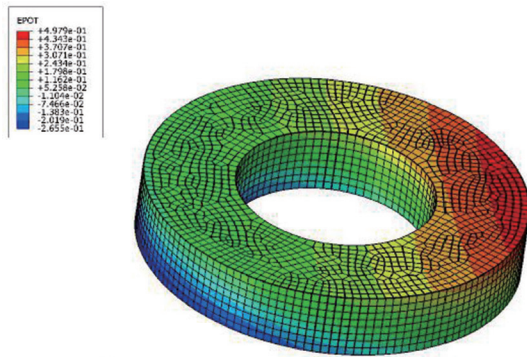

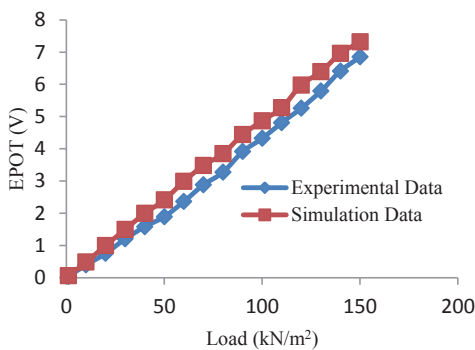Fig. 9. Electrical potential (V) transformation of the BaTiO$_3$ specimen in ABAQUS.

and simulation results for this material under the variable loads; we observed that the EPOT (V) changed significantly with the load changes. We also observed linear behavior between two parameters. The linear dependence of V on loading must be understood given the fact that more mechanical work is performed at maximum loading conditions. That is, the mechanical work performed by piezoelectric material is directly related to the area under load-displacement curves. The main outcome of this analysis was that the V increased with increased loading, which shows that the material's efficiency increased nearly linearly when we increased the loads. We found the measured error between the experimental and simulation results to be less than 7%.

3.4 Structural dynamic analysis

In this phase, we conducted a dynamic analysis that entailed applying a constant load of 10 kN/m^2 to the top layer and generating the corresponding V. We detected the natural frequency of the material experimentally by tracing the maximum electrical potential, and the harvester produced the maximum electric potential at this frequency. We excited the harvester using a shaker at a certain frequency with constant amplitude. We identified the resonant frequency by observing the maximum output voltage as a function of excitation frequency under certain excitation levels. We used the function generator to provide excitation frequency that varied from 1 to 100 Hz.

Figure 11 shows the generated output voltage distribution, which depends on the loading frequency of the piezoelectric material. The V increased as loading frequency increased from 1 Hz to 35 Hz. Figure 11 shows that the maximum EPOT (5.37 V) experimentally at 10 kN/m^2 across a 35 Hz resonance frequency. The corresponding value that we calculated in ABAQUS under the same loading condition was 6.43 V at 35 Hz resonance frequency. We observed that the frequencies of the peak output voltages were nearly the same as the resonant frequency of the piezoelectric element that we identified using the experimental setup; the output voltage reached its maximum value under this excitation frequency. The V went off when the excited frequency diverged from the resonant frequency. We obtained the maximum electric potential across the harvester when the natural frequency matched the resonance frequency of the vibration source, and the resonance frequency changed when we changed the load. As we knew, at constant amplitude, the resonance frequency is inversely proportional to the square root of the effective mass. When we increased the load, the resonance frequency decreased nonlinearly. The EPOT estimated in the simulation model correlated well with what we found in the laboratory experiment.
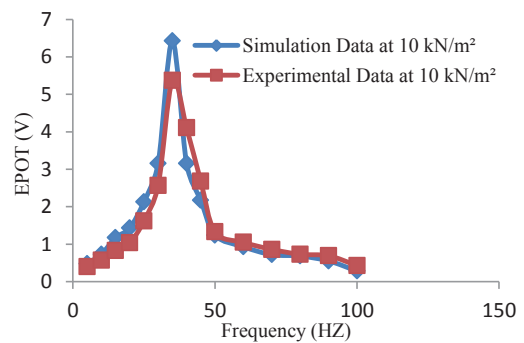

Fig. 10. Comparison between the experimental and simulation results under static loading conditions.

Fig. 11. Comparison between the experimental and simulation results of BaTiO$_3$ at 10 kN/m^2 under variable frequency.

168

Trans. Electr. Electron. Mater. 18(3) 163 (2017): Z. Butt *et al.*

4. CONCLUSIONS

The present work aimed to establish the validity of an energy-harvesting system by using commonly available BaTiO$_3$ piezoelectric material. Our objective was to find the most efficient, reliable, and precise FE package. With that goal, we used commercially available finite element software, ABAQUS, to carry out the structural-electrical analysis of this material. From the analysis, we reached the following conclusions:

1. Microscopic study showed the presence of some agglomeration and heterogonous distribution of grains all over the substrate. Energy-dispersive x-ray analysis showed that there were no impurities in the material we selected for the required analysis.
2. The piezoelectric energy harvester showed increased polarization rates under higher vibrating load conditions and hence increased electric potential. As a result, we observed linear behavior, and the material showed optimum performance under a static load with an error of less than 7% between the experimental and simulation values.
3. We obtained the maximum EPOT at the resonance frequency of 35 Hz and then decayed rapidly under dynamic loading. The % error between the experimental and simulation results was approximately 5%.
4. By correlating the simulation and experimental values, we observed that FEA was useful for precisely foreseeing the behavior of the BaTiO$_3$ material under static and dynamic loading conditions.

ACKNOWLEDGMENT

REFERENCES

[1] Z. Xiao, T. Q. Yang, and Y. Dong, *Appl. Phys. Lett.*, **104**, 223904 (2014).
[2] Z. Butt, R. A. Pasha, F. Qayyum, Z. Anjum, and H. Elahi, *J. Mech. Sci. Technol.*, **30**, 3553 (2016).
[3] S. Wang, K. H. Lam, C. L. Sun, K. W. Kwok, M. S. Guo, and X. Z. Zhao, *Appl. Phys. Lett.*, **90**, 11350 (2007). [DOI: http://dx.doi.org/10.1063/1.2713357]
[4] Z. Butt and R. A. Pasha, *IOP Conf. Ser., Mater. Sci. Eng.*, **14601** (2016).
[5] X. R. Chen, T. Q. Yang, W. Wang, and X. Yao, *Ceramics International*, **38S**, S271 (2012).
[6] F. Qayyum, M. Shah, S. Manzoor, and M. Abbas, *Mater. Sci. Technol.*, **31**, 317 (2015).
[7] Z. Anjum, F. Qayyum, S. Khushnood, S. Ahmed, and M. Shah, *Materials and Design*, **87**, 750 (2015).
[8] M. W. Lin, *J. Intell. Material Sys. And Structures*, **5**, 869 (1994).
[9] W. S. Hwang and H. C. Parket, *AIAA J.*, **31**, 930 (1993).
[10] A. H. Allik and J. R. Hughes, *Int. J. Num. Methods Eng.*, **2**, 151 (1970).
[11] R. Lerch, *IEEE Trans. Ultrasonics Feroelectr. Frequency Control*, **37**, 233 (1990).
[12] D. H. Wu, W. T. Chien, C. J. Yang, and Y. T. Yen, *Sensor. Actuat. A*, **118**, 171 (2005).
[13] C.D.M. Junior and A. Erturk, *Journal of Sound and Vibration*, **327**, 9 (2009).
[14] F. Lowrie, *National Physics Laboratory* (Teddington, Middlesex, UK, 1999).
[15] M. Staworko and T. Uhl, *MECHANICS*, **27**, 4(2008).
[16] J. A. Venables and C. J. Harland, *Philosophical Magazine*, **27**, 1193 (1973).
[17] X. Wu, X. Pan, and J. F. Stubbins, *J. Nucl. Mater.*, **361**, 228 (2007).
[18] P. Hortolà, *Micron 41*, **7**, 904 (2010).
[19] M.N.G. Nejhad and S. Pourjalali, *J. of Thermoplast. Compos. Mater.*, **19**, 309 (2006).
[20] A. E. Giannakopoulos and S. Suresh, *Acta Mater*, **47**, 2153 (1999).
[21] G. H. Haertling, *J. Am. Ceramic Soc.*, **82**, 797 (1999).
[22] O. Khalid, Z. Butt, W. Tanveer, and H. I. Rao, *Heat Mass Transf.*, **53**, 1391 (2017). [DOI: http://dx.doi.org/10.1007/s00231-016-1914-2]